Available online at www.sciencedirect.com
SCIENCE DIRECT®
Sensors and Actuators B 99 (2004) 66–73
SENSORS AND ACTUATORS B CHEMICAL
www.elsevier.com/locate/snb

# High-pressure electroosmotic pumps based on porous polymer monoliths

Jennifer A. Tripp [a], Frantisek Svec [a,*], Jean M.J. Fréchet [a,1], Shulin Zeng [b], James C. Mikkelsen [b], Juan G. Santiago [b]

[a] *Department of Chemistry, University of California, Berkeley, CA 94720-1460, USA*
[b] *Department of Mechanical Engineering, Stanford University, Stanford, CA 94305, USA*

Received 6 June 2003; received in revised form 27 October 2003; accepted 30 October 2003

**Abstract**

Electroosmotic pumps have been prepared using macroporous polymer monoliths with their pore surface grafted with the ionizable monomers 2-acrylamido-2-methyl-1-propanesulfonic acid and [2-(methacryloyloxy)ethyl]trimethyl ammonium chloride, respectively. The effects of critical parameters such as pore size of the monolith, percentage of ionizable moieties in the grafted layer, crosslinking density, and driving voltage on both flow rate and pressure have been quantified. Electroosmotic pumps fabricated from the grafted monoliths afforded pressures as high as 0.38 MPa and electric-field-specific flow rates of up to 0.41 ml/min, both at an applied potential of 50 V.


*Keywords:* Electroosmotic pumps; Porous; Polymer; Monolith

## 1. Introduction

Many assay systems [1,2] require that liquid samples flow through channels of the microfluidic system. A variety of approaches to liquid driving devices suitable for microfluidics has been demonstrated and can be divided into two categories: (i) membrane displacement and (ii) field-induced pumps [3]. Electroosmotic pumping is an important sub-class of the latter category and is being widely used in the field of μ-TAS [3–11]. Electroosmotic pumps do not require mechanical moving parts and can generate flow rates and pressures superior to those afforded by other technologies. Numerous electroosmotic channel systems and pumps have been fabricated using fused silica capillaries [4], long glass channels [9], short pumping slots etched in glass or silicon [7,8], disks from sintered glass particles [10], and tubes packed with silica beads, all containing ionizable surface functionalities [3].

Some of the current devices that generate electroosmotic flow (EOF) utilize particulate structures such as beads in order to achieve the desired high surface-to-volume ratio required for efficient electroosmotic pumping. However, packing beads with a diameter of several micrometers or less into microchannels of complex devices is difficult and anchoring them at specific locations requires additional fabrication steps [12,13]. In contrast, porous polymer monoliths can be prepared in situ by a simple polymerization from liquid precursors including monomers, crosslinker, free radical initiator and porogenic solvent [14]. The monolith, which is a single continuous piece of highly crosslinked porous polymer, completely fills the volume of a specifically designed chamber or a section of the microfabricated channel. The characteristic pore dimension of the monolith can be controlled over a broad range of 0.01–10 μm by altering the composition of the porogenic solvent, the percentage of crosslinking monomer in the polymerization mixture, and the polymerization temperature. Since their introduction in the early 1990s [15], monolithic materials have been successfully used in a wide variety of applications [16–18] including capillary electrochromatography with EOF as the flow driving force [19–22].

Recently, we have used inert porous polymer monoliths as frits or filters that hold beds of silica particles to fabricate large-bore electroosmotic pumps [23]. Our previous work also indicated that the size and porosity of the beads might be critical to pump performance [3]. Since the preparation of porous monoliths is simple and their porous properties and surface chemistry is easily controlled, they are ideally

* Corresponding author. Tel.: +1-510-643-3168; fax: +1-510-643-3079.
*E-mail address:* svec@uclink4.berkeley.edu (F. Svec).
[1] Co-corresponding author.

0925-4005/$ – see front matter © 2003 Elsevier B.V. All rights reserved.
doi:10.1016/j.snb.2003.10.031

suited to study the effect of pore size on the generation of pressure in EO pumps. This report describes the fabrication of electroosmotic pumps using porous polymer monoliths with grafted ionizable functionalities and effects of material properties on their performance.

## 2. Theory of electroosmotic pumping

Eq. (1) relates the flow rate $Q$ achieved using a pump containing electroosmotically active porous structure to the generated pressure $\Delta P$ [3]:

$$Q = \frac{\psi \Delta P A a^2}{8\mu L\tau} - \frac{\psi \varepsilon \zeta V A}{\mu L \tau}\left(1 - \frac{2\lambda I_1(a/\lambda)}{aI_0(a/\lambda)}\right) \quad (1)$$

In this equation, $A$ is the cross-sectional area of the pump, $a$ the characteristic pore radius, $L$ the length of the pump, $\zeta$ the zeta potential of the monolithic polymer, and $V$ is the voltage used to actuate the pumping. Specific characteristics of the working fluid include the viscosity, $\mu$, and the dielectric constant, $\varepsilon$. The tortuosity $\tau$ is defined as $\tau = (L_e/L)^2$, where $L_e$ is the average path length of a fluid particle through the device and $L$ is the length of the pump. The porosity $\psi$ is defined as the ratio of the void volume, $U_e$, to the total volume of the porous structure, $U$. Eq. (1) states that the net flow produced by the device is a linear superposition of the pressure driven flow component (first term) and the EOF (second term).

Solving Eq. (1) for $\Delta P_{max}$ affords the following relation:

$$\Delta P_{max} = \frac{8\varepsilon\zeta V}{a^2}\left(1 - \frac{2\lambda I_1(a/\lambda)}{aI_0(a/\lambda)}\right) \quad (2)$$

For high values of $a/\lambda$, the term in parentheses is unity and the maximum pressure is proportional to the geometrical factor $1/a^2$. At values of $a/\lambda$ of unity and below, the finite effects of electrical double layers can result in pressures, which fall well below the ideal value of $8\varepsilon\zeta V/a^2$. Since most of the terms of Eq. (1) are fixed for a specific working liquid, a primary design parameter is the zeta potential, $\zeta$, which Smoluchowski [24,25] defined as

$$\zeta = \frac{\sigma\delta}{\varepsilon_o \varepsilon_r} \quad (3)$$

In this expression, derived from a simple capacitor model for the field in an electrical double layer, $\sigma$ is the surface charge and $\delta$ is the characteristic thickness of the double layer. Eq. (3) is an approximate relation, which is most accurate when $\delta$ equals the Debye length of the electrolyte solution, $\lambda$, and for the case of low thermal, energy specific potentials, $ze\zeta/kT \ll 1$, where $z$ is the valence of the double layer ions and $e$ is the charge of an electron. Zeng et al. [3] have suggested that optimum values of pore size and buffer composition must be found in order to achieve best results with any given pump. For example, high ionic strength of the electrolyte leads to a decrease in $\lambda$, thus enabling higher values of $a/\lambda$ for a given geometry. Simultaneously, pressure capacities are approaching the ideal value. However, more Joule heat is generated at high ionic strength which is reflected in a decrease in thermodynamic efficiency.

## 3. Experimental methods and setup

### 3.1. Materials

All monomers shown in Fig. 1, porogenic solvents, and initiators were purchased from Aldrich and used as supplied, with the exception of 4,4′-azobis(4-cyanovaleric acid) (ACVA), which was purified by extraction with diethyl ether in a Soxhlet apparatus. Water was purified by reverse osmosis and deoxygenated by purging with nitrogen gas for 20 min prior to use.

### 3.2. Preparation of poly(chloromethylstyrene-co-divinylbenzene) monoliths

A detailed procedure for the preparation of the monoliths has been described elsewhere [26]. Briefly, a monolith with a pore size of 1700 nm was prepared using a solution of 2,2′-azobisisobutyronitrile (0.12 g, 1 wt.% with respect to monomers) in chloromethylstyrene (4.8 g), divinylbenzene (80% grade, 7.2 g), toluene (5.25 g) and 1-dodecanol (12.75 g). The mixture was purged with nitrogen for 10 min, poured into a mold, which is a glass tube with an inner diameter of 14 mm sealed at one end, and the open end of the mold was sealed. The inner walls of this tube were lined with shrinkable polyethylene tubing. The polymerization was allowed to proceed in a thermostated bath for 20 h at 70 °C. The glass tube was then carefully crushed and stripped away, and the monolith, encased in polyethylene tubing, was sliced into 1 cm thick disks. These disks were extracted with tetrahydrofuran (THF) for 24 h in a Soxhlet apparatus to remove the porogenic solvent from the pores.

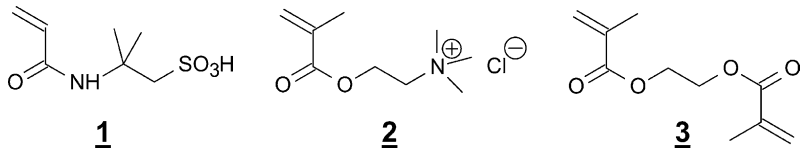


1 2 3

Fig. 1. Structures of monomers used for grafting: 2-acrylamido-2-methyl-1-propanesulfonic acid) 1, [2-(methacryloyloxy)ethyl]trimethylammonium chloride 2, and ethylene dimethacrylate 3.

### 3.3. Attachment of 4,4′-azobis(4-cyanovaleric acid) to pore surface

Several monolithic poly(chloromethylstyrene-co-divinylbenzene) disks were added to a solution of 3.0 g ACVA and 2.0 g triethylamine in 6.0 ml *N*,*N*-dimethylformamide. The reaction was carried out with no stirring at room temperature for 48 h. The modified disks were then washed with diethyl ether in a Soxhlet extractor for 24 h. For characterization purposes and prior to elemental analysis of nitrogen, the monolithic disks were submerged in toluene and heated to 70 °C for 20 h to remove diazo functionalities of the attached initiator, followed by washing with THF. Elemental analysis after this heating reveals 0.69% nitrogen residing in the nitrile groups, corresponding to 0.5 mmol/g. This amount represents only those initiating species that are attached to the pore surface of the monolith.

### 3.4. Grafting of ionizable monomers

An aqueous solution of the 2-acrylamido-2-methyl-1-propanesulfonic acid (AMPS) (1) or [2-(methacryloyloxy) ethyl]trimethylammonium chloride (META) (2), and ethylene dimethacrylate (EDMA) (3) (1 or 2 wt.% with respect to functional monomer 1 or 2), was purged first in a flask with nitrogen for 10 min. A monolithic disk functionalized with ACVA was submerged in this solution, the flask sealed, and heated to 70 °C for 20 h. The soluble polymer was removed from the grafted disks by extraction with THF in a Soxhlet apparatus for 24 h. Polymer gel that might be attached to the face surfaces of the monolith was removed manually.

### 3.5. Methods

Pore size distribution measurements were performed using an Autopore III mercury intrusion porosimeter (Micromeritics, Norcross, GA). Infrared spectra were monitored using Mattson Genesis II FTIR spectrometer (Fremont, CA).

All EOF and pressure measurements were carried out using a home-made apparatus described in detail in [3] and shown in Fig. 2. This unit consists of an acrylic frame onto which the monolithic pumping structures were mounted, an acrylic housing fitted with inlet and outlet fluidic connections, and platinum electrodes. In the case of negatively charged polymers, oxygen gas generated at the upstream/anode side of the device was vented to the atmosphere and hydrogen gas bubbles generated at the cathode exited through the fluidic outlet port. Note that, in the experimental configuration for maximum pressure measurement, hydrogen gas was allowed to accumulate at the pump outlet (on the side of the pressure transducer). At near-steady conditions, this volume flux of hydrogen gas on the outlet side results in a small negative flow rate of liquid through the pump (in the direction opposite to the field for negative zeta potentials). Thus, the pump pressure capacity obtained from the measurement tends to overestimate the actual value. The degree to which pressure is overestimated due to hydrogen gas flow rate can be calculated using a simple pump model. The ratio of hydrogen-to-liquid volume flow rate in the pump can be obtained using the following relation [27]:

$$\frac{Q_{H_2}}{Q_{liquid}} = \frac{IkT}{2ePQ_{liquid}} \quad (4)$$

where $Q_{H_2}$ is the volume flow rate of hydrogen at a gas phase temperature $T$ and pressure $P$, $Q_{liquid}$ is the pumping flow rate for the liquid, and $I$ is the total current supplied to the system. For the maximum pressure measurements shown in Table 2, the ratio of hydrogen flow rate (at the high pressure condition) to the flow rate of liquid across the pump was 30%. The measured maximum pressures represents then about 75% of the actual pump pressure capacity. It is worth

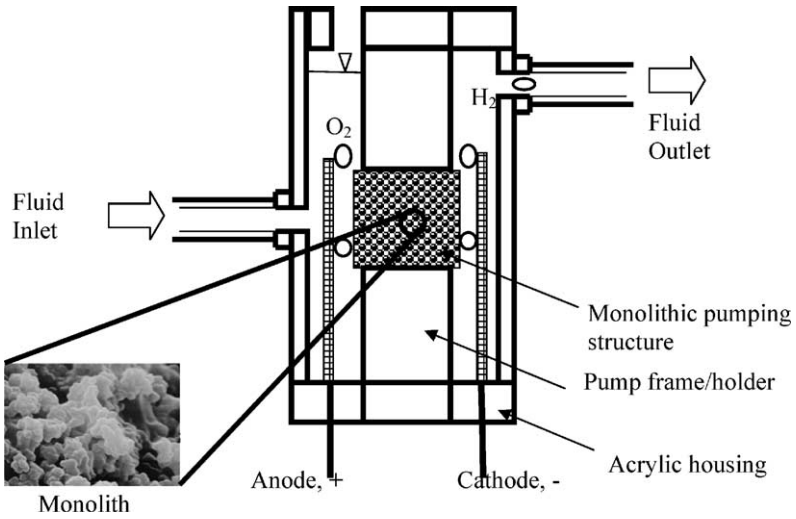


Fig. 2. Schematic of experimental unit used for measuring the electroosmotic pumping capabilities of monolithic disks. Flow direction is shown for a pump incorporating a disk with a negatively charged surface grafted with 2-acrylamido-2-methyl-1-propanesulfonic acid.

of noting that these conservative estimates of gas flow rates neglect gas dissolution into the electrolyte, which may be significant. In all pumping experiments, the electrolyte solution consisted of a 0.5 mol/l borate buffer pH 9.2 and a concentration of sodium ions of 1.0 mmol/l. This buffer affords a theoretical Debye length λ of 9.6 nm.

## 4. Results and discussion

### 4.1. Preparation of functionalized monoliths via copolymerization

The direct copolymerization of functional monomers would presumably constitute the simplest approach to monolithic polymers containing ionizable functionalities. However, our initial attempts to prepare monoliths using this technique were not successful, since we could not find a porogenic system that dissolved all of the components of the polymerization mixture while enabling the formation of monoliths with pore sizes in the desired range. Although pumps fabricated from these less than perfect monoliths generated EOF, the electric current we monitored was unacceptably high and excessive Joule heating was observed. This is likely due to a poor copolymerization process resulting from unfavorable reactivity ratios of the various monomers. As a result, most of the ionizable groups were buried within the inaccessible polymer mass rather than being exposed at the pore surface. While charged groups buried under a neutral polymer dielectric can still contribute to the electric field required for the formation of an electrical double layer and therefore also EOF, this configuration may significantly inhibit the ionization process itself and result in fewer surface-bound charges, which drives EOF. Taking these difficulties into account, we decided to abandon this method in favor of a surface grafting approach.

### 4.2. Surface grafting

Grafting enables the controlled introduction of ionizable functionalities onto the surface of pores located throughout the monolith. Our process is shown in Fig. 3. First, a "generic" monolith containing benzyl chloride functionalities **4** is prepared by polymerization of chloromethylstyrene and divinylbenzene in the presence of a toluene–dodecanol mixture that serves as a porogen. Monoliths varying in pore sizes were prepared from mixtures summarized in Table 1.

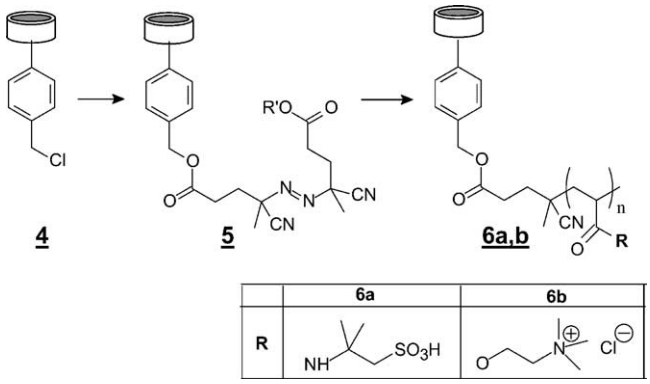


Fig. 3. Scheme illustrating modification reactions affording monolithic disks with ionizable functionalities grafted from the pore surface.

The proportion of toluene and dodecanol in the porogenic mixture efficiently controls the pore size. Fig. 4 shows the pore size distribution profiles of the three monoliths used in this study. Since the pore size is controlled only by altering the proportion of toluene and dodecanol in the polymerization mixture, while keeping the percentage of both monomers fixed, the overall chemical composition of the polymers does not change. This feature suggests that the density of reactive functionalities located at the surface can be assumed to remain constant despite the pore size variations.

In the second step, a free radical initiator, 4,4′-azobis(4-cyanovaleric acid), containing latent nucleophilic carboxylic acid functionalities is attached to the surface of electrophilic monolithic disks 4 to form monolith 5 with ester linkages between the surface and the radical initiator moieties. These monoliths are then immersed in a solution of a commercially available ionizable monomers (AMPS 1 or META 2) and the grafting polymerization is initiated by heating to afford monoliths **6a** and **6b**, respectively, with chains of ionizable moieties covalently attached to the surface.

A small percentage of a crosslinker (EDMA, 3) is added to the mixture to increase the grafting efficiency and to ensure full incorporation of most of the available monomers into the grafted layer [26]. The percentage of crosslinker used also controls swelling of the grafted polymer and therefore also the flow-through properties of the final disk. We have also found in our previous work that the number of functional moieties attached to the pore surface is proportional to the concentration of the specific monomer in the grafting solution [28,29].

Table 1
Compositions of polymerization mixtures used for the preparation of reactive porous polymer monoliths with controlled porous properties

| Entry | CMS (g) (%)[a] | DVB (g) (%)[a] | AIBN (g)[a] | TOL (g) (%)[a] | DoOH (g) (%)[a] | $D_p$ (nm)[b] | Porosity (%)[b] |
|---|---|---|---|---|---|---|---|
| 1 | 4.8 (16) | 7.2 (24) | 0.12 | 5.80 (19.3) | 12.20 (40.7) | 460 | 56 |
| 2 | 4.8 (16) | 7.2 (24) | 0.12 | 5.45 (18.1) | 12.55 (41.9) | 970 | 60 |
| 3 | 4.8 (16) | 7.2 (24) | 0.12 | 5.25 (17.5) | 12.75 (42.5) | 1700 | 48 |

[a] CMS: chloromethylstyrene; DVB: divinylbenzene; AIBN: 2,2′-azobisisobutyronitrile; TOL: toluene; DoOH: 1-dodecanol.
[b] Median pore diameter $D_p$ and porosity determined by mercury intrusion porosimetry.

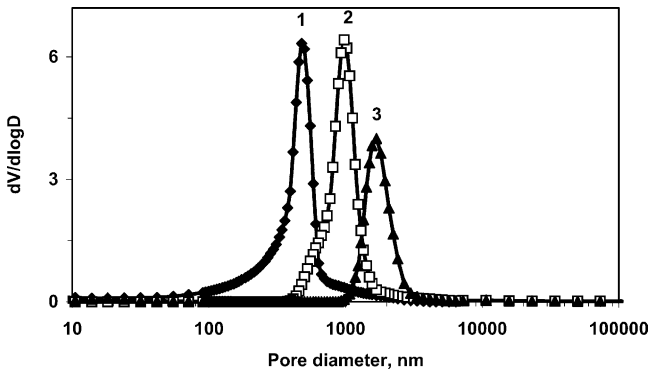


Fig. 4. Pore size distribution profiles of chloromethylstyrene–divinylbenzene monoliths used in this study. *Conditions*: polymerization mixture—chloromethylstyrene 16%, 80% grade divinylbenzene 24%, 2,2′-azobisisobutyronitrile 1% with respect to monomers, porogenic solvent (mixtures of 1-dodecanol and toluene) 60%; temperature 70 °C; time 20 h; percentage of toluene in polymerization mixture 19.3% (1, ◆), 18.1% (2, □), and 17.5% (3, ▲).

After ionization, monoliths with grafted chains originating from monomer 1 possess a negatively charged surface, which supports EOF toward the cathode, just like analogous pumps that use silica particles with weakly acidic silanol functionalities to drive the flow [3,23]. In contrast, monomer 2 leads to positively charged surfaces affording anodic EOF.

### 4.3. Electroosmotic pumping

The assembly shown in Fig. 2 enables the rapid testing of the pumping function of grafted monolith disks. Using this unit, we varied the applied potential to assess the effect of pore size, monomer and crosslinker concentrations in the grafting solution, as well as the sign of the charge (positive or negative) of the pore surface on flow, pressure, and current of the pump.

Fig. 5 shows the pressure versus flow rate performance of two monolithic pumping devices. As predicted by Eq. (1),

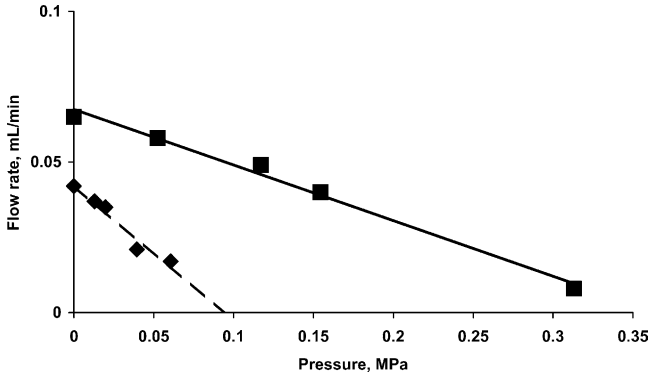


Fig. 5. Effect of percentage of ethylene dimethacrylate in the grafting solution containing 2-acrylamido-2-methyl-1-propanesulfonic acid on the performance of the electroosmotic pump at a voltage of 100 V. *Grafting conditions*: monolith length 1 cm, diameter 1.3 cm, pore size 1700 nm; 5% aqueous solution of 2-acrylamido-2-methyl-1-propanesulfonic acid containing 1% (■) or 2% (◆) ethylene dimethacrylate; grafting temperature 70 °C for 20 h.

Table 2
Effect of monomer solution concentration and percentage of crosslinker on flow and pressure characteristics of disks grafted with 2-acrylamido-2-methyl-1-propanesulfonic acid

| Pore size (nm) | $C_{sol}$ (%)[a] | $C_{EDMA}$ (%)[b] | $\Delta P_{max}$ (MPa)[c] | $Q_{max}$ (ml/min)[d] |
|---|---|---|---|---|
| 460 | 5 | 1 | 0.18 | 0.23 |
| 460 | 5 | 2 | 0.13 | 0.08 |
| 460 | 10 | 1 | 0.33 | 0.11 |
| 460 | 10 | 2 | 0.38 | 0.05 |
| 970 | 5 | 1 | 0.006 | 0.16 |
| 970 | 5 | 2 | 0.04 | 0.31 |
| 970 | 10 | 1 | 0.026 | 0.15 |
| 970 | 10 | 2 | –[e] | 0.28 |
| 1700 | 5 | 1 | 0.019 | 0.40 |
| 1700 | 5 | 2 | 0.013 | 0.41 |
| 1700 | 10 | 1 | 0.036 | 0.33 |
| 1700 | 10 | 2 | 0.018 | 0.34 |

[a] $C_{sol}$: concentration of monomer in grafting solution.
[b] $C_{EDMA}$: concentration of crosslinker with respect to monomer in grafting solution.
[c] $\Delta P_{max}$: maximum pressure generated at 50 V.
[d] $Q_{max}$: maximum flow rate at 50 V.
[e] Measurement cannot be carried out due to excessive current.

the plots are linear. For example, the monolith with a pore size of 1700 nm grafted with a mixture consisting of 5% AMPS and 1% EDMA affords flow rates of up to 0.41 ml/min or a maximum pressure of over 0.03 MPa at a potential of 100 V. Our results also show that pump performance depends on the crosslinking of the grafted ionizable layer. In contrast to the previous 1% crosslinked layer, both the pressure capacity and maximum flow rate are significantly reduced for a monolith grafted with a mixture containing 2% EDMA. Table 2 summarizes effects of the three variables we studied on maximum pump pressure and flow rate that can be achieved with the pump. As predicted by theory, the highest pressure of over 0.38 MPa is achieved with the pump assembled using monolith with the smallest pores (460 nm), which has a $a/\lambda$ value of 48.

A lower percentage of EDMA in the grafting mixture results in a less crosslinked gel that swells to a higher degree and fills the pore volume to a greater extent. As a result, the effective pore diameter is smaller. These apparently smaller pores then generate a higher pressure. Fig. 6 illustrates this effect schematically. Table 2 also shows that in contrast to the devices with small pores generating the highest pressures, it is the monolith with the largest pores that affords the highest flow rate of 0.41 ml/min.

Eq. (1) implies that the flow rate depends on the applied potential $V$. Indeed, Fig. 7 shows that $\Delta P_{max}$ increases with the voltage up to an applied potential of 150 V. Thereafter, the generated pressure exceeds that predicted by Eq. (1) and an increase in current is also observed (Fig. 7). This may result from differences in swelling of the grafted polymer layer at the higher temperature as a result of the Joule heat generated, which further restricts pore size thus increasing the generated pressure. Fig. 7 also shows the importance

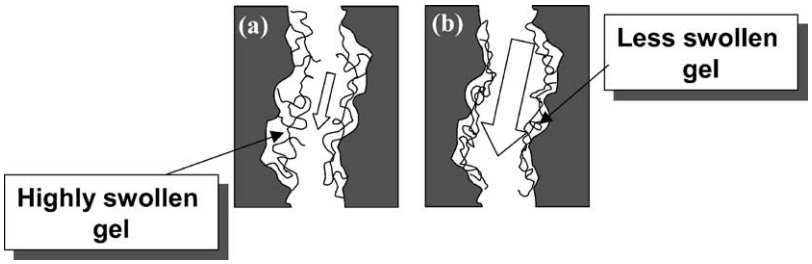


Fig. 6. Schematic of proposed model describing the effect of crosslinking density on pore size. A less crosslinked gel (a) swells and fills the pore to a higher degree, thus reducing the effective pore size. A more crosslinked gel (b) swells less, leaving the pore more open. Reducing the amount of crosslinker leads to a decrease in the effective pore size. The pump then generates a higher pressure.

of temporal responses of the pump to changes in applied potential, which is currently under investigation.

As suggested by the simple model of Eq. (3), the $\zeta$ potential is proportional to the charge density, $\sigma$. This suggests that a larger amount of grafted ionizable polymer should lead to an increase in $\zeta$ and therefore to an increase in flow rate per unit of electric field. However, our results do not support this simple prediction. As shown in Table 2, the flow rates generated by monoliths grafted with a 5% solution are higher or equal to those grafted with solutions that contain 10% monomer. Since practically all monomers present in these solutions are converted to a grafted polymer, the latter disks contain twice as much grafted polymer. As a result, these discs also contain twice the number of ionizable functionalities. However, it is likely that the ionized functionalities of this gel layer are in close proximity at a distance shorter than the thickness of the double layer. As a result, the double layers of these functionalities may overlap and the driving force is reduced. This is macroscopically translated into a decrease in flow rate.

Eqs. (1) and (2) indicate that the polarity of the surface charge determines the polarity of the $\zeta$ potential, which, in turn, controls the flow direction within the porous structure. This is illustrated on monoliths grafted with monomers of opposite polarities. Table 3 compares the flow and pressure achieved with pumps using monoliths grafted with META and AMPS, respectively. Indeed, no significant difference in performance is observed aside from flow direction. However, the current densities per unit of electric field monitored for the disks grafted with META are about half of those found for AMPS monoliths. This appears to result from the properties of the counterions of ionized META. These mobile counterions in the electrical double layers are borates that afford lower current in the double layer. In contrast, the AMPS counterions are protons or (mostly) sodium cations, which have higher mobility and therefore generate higher current. This difference can be substantial since the current generated in the electrical double layer may represent a significant portion of the total current [30]. The low current and highly efficient operation found for the monolithic

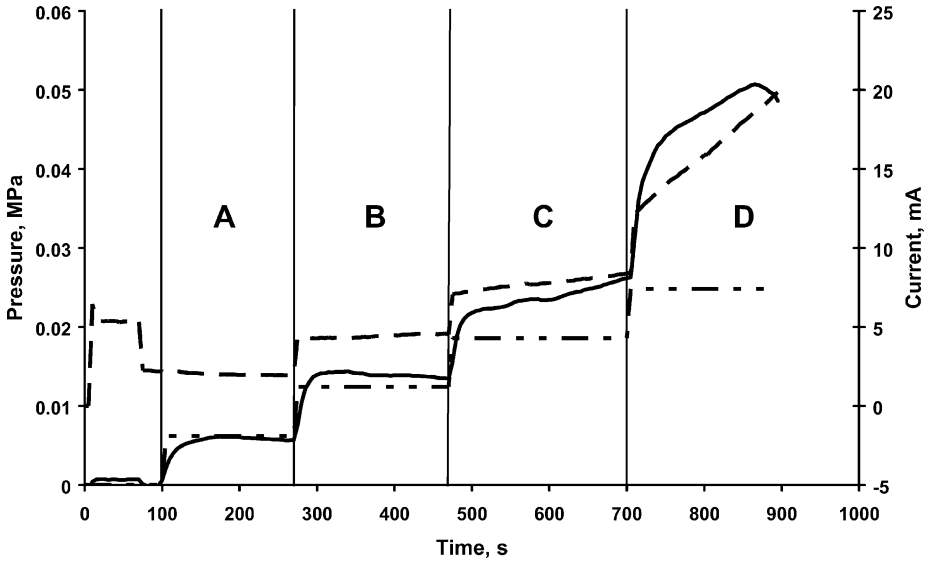


Fig. 7. Effect of voltage on generation of pressure and current in the monolithic pump. *Grafting conditions*: monolith length 1 cm, diameter 1.3 cm, pore size 1700 nm; 5% aqueous solution of 2-acrylamido-2-methyl-1-propanesulfonic acid containing 1% ethylene dimethacrylate with respect to AMPS. Applied voltage—part A, 50 V; part B, 100 V; part C, 150 V; and part D, 200 V. Full line represents the observed pressure, the dashed line measured current, and the dashed-dotted line represents ideal fast response as calculated by scaling the initially observed pressure with applied voltage.

Table 3
Flow, and pressure characteristics of disks grafted with 2-acrylamido-2-methyl-1-propanesulfonic acid (AMPS) and [2-(methacryloyloxy)ethyl] trimethylammonium chloride (META)[a]

| | Pore size 460 nm, EDMA 2% | | Pore size 1700 nm, EDMA 1% | |
|---|---|---|---|---|
| | $Q_{max}$ (ml/min) | $\Delta P_{max}$ (Mpa) | $Q_{max}$ (ml/min) | $\Delta P_{max}$ (MPa) |
| META[b] | −0.03 | −0.15 | −0.30 | −0.02 |
| AMPS | 0.08 | 0.13 | 0.40 | 0.02 |

[a] Disk: 13 mm diameter × 10 mm thick with a pore size of 460 or 1700 nm grafted with 5% solution of AMPS or META containing 1 or 2% ethylene dimethacrylate with respect to functional monomer.

[b] Flow and pressure generation of META-grafted monoliths were in the opposite direction with respect to the applied electric field compared to monoliths grafted with AMPS.

pump grafted with META is very promising for the future development of pumping devices employing EOF.

## 5. Conclusions

Monolithic disks prepared from a porous polymer with grafted ionizable functionalities can be used as the active elements of electroosmotic pumps. Since the pore size and pore volume of the monolith, as well as the properties of the grafted layer such as its chemistry, thickness, and crosslinking density can be easily controlled, a variety of pumping devices can be prepared to achieve the desired flow direction, flow rate, and pressure. Although our concept is demonstrated with macroscopic pumps, the ease of preparation of these discs from liquid precursors makes this approach well suited for the fabrication of pumping devices inside capillaries or microfluidic chip channels.

## Acknowledgements

This work was supported by grant from DARPA (F30602-00-1-0571), with Michael Krihak as program director. Additional support from the National Institute of General Medical Sciences, National Institutes of Health (GM-48364) and the Office of Nonproliferation Research and Engineering of the US Department of Energy under contract no. DE-AC03-76SF00098 is also gratefully acknowledged.

## References

[1] D.R. Reyes, D. Iossifidis, P.A. Auroux, A. Manz, Micro total analysis systems. 1. Introduction, theory, and technology, Anal. Chem. 74 (2002) 2623–2636.
[2] P.A. Auroux, D. Iossifidis, D.R. Reyes, A. Manz, Micro total analysis systems. 2. Analytical standard operations and applications, Anal. Chem. 74 (2002) 2637–2652.
[3] S. Zeng, C.-H. Chen, J.C. Mikkelsen, J.G. Santiago, Fabrication and characterization of electroosmotic micropumps, Sens. Actuators B: Chem. 79 (2001) 107–114.
[4] P.K. Dasgupta, S. Liu, Electroosmosis: a reliable fluid propulsion system for flow injection analysis, Anal. Chem. 66 (1994) 1792–1798.
[5] H. Salimi-Moosavi, T. Tang, D.J. Harrison, Electroosmotic pumping of organic solvents and reagents in microfabricated reactor chips, J. Am. Chem. Soc. 119 (1997) 8716–8717.
[6] K. Morishima, D.W. Arnold, A.R. Wheeler, D.J. Rakestraw, R.N. Zare, Novel separation method on a chip using capillary electrochromatography in combination with dielectrophoresis, in: Proceedings of the 219th ACS National Meeting, San Francisco, CA, 26–30 March 2000, p. 466.
[7] C.-H. Chen, J.G. Santiago, A planar electroosmotic micropump, JMEMS 11 (2002) 672–683.
[8] D. Laser, K.E. Goodson, J.G. Santiago, T.W. Kenny, Impact of pumping surface separation distance on micromachined electroosmotic pump performance, in: Proceedings of the International Mechanical Engineering Congress and Exposition, 6th Micro-Fluidic Symposium, MEMS-23876, Proceedings vol. 2, New York, 2001.
[9] W.E. Morf, O.T. Guenat, N.F. de Rooij, Partial electroosmotic pumping in complex capillary systems. Part 1. Principles and general theoretical approach, Sens. Actuators B: Chem. 72 (2001) 266–272.
[10] W. Gan, L. Yang, Y. He, R. Zeng, M.L. Cervera, M. de la Guardia, Mechanism of porous core electroosmotic pump flow injection system and its application to determination of chromium(VI) in waste-water, Talanta 51 (2000) 667–675.
[11] T.E. McKnight, C.T. Culbertson, S.C. Jacobson, J.M. Ramsey, Electroosmotically induced hydraulic pumping with integrated electrodes on microfluidic devices, Anal. Chem. 73 (2001) 4045–4049.
[12] R.D. Oleschuk, L.L. Shultz-Lockyear, Y.B. Ning, D.J. Harrison, Trapping of bead-based reagents within microfluidic systems: on-chip solid-phase extraction and electrochromatography, Anal. Chem. 72 (2000) 585–590.
[13] A.B. Jemere, R.D. Oleschuk, F. Ouchen, F. Fajuyigbe, D.J. Harrison, An integrated solid-phase extraction system for sub-picomolar detection, Electrophoresis 23 (2002) 3537–3544.
[14] F. Svec, J.M.J. Fréchet, New designs of macroporous polymers and supports: from separation to biocatalysis, Science 273 (1996) 205–211.
[15] F. Svec, J.M.J. Fréchet, Continuous rods of macroporous polymer as high-performance liquid chromatography separation media, Anal. Chem. 64 (1992) 820–822.
[16] F. Svec, J.M.J. Fréchet, Molded rigid monolithic porous polymers: an inexpensive, efficient, and versatile alternative to porous beads for the design of materials with high flow characteristics for numerous applications, Ind. Eng. Chem. Res. 36 (1999) 34–48.
[17] F. Svec, E.C. Peters, D. Sýkora, J.M.J. Fréchet, Design of monolithic polymers used in capillary electrochromatography columns, J. Chromatogr. A 887 (2000) 3–30.
[18] F. Svec, J.M.J. Fréchet, R.W. Allington, S. Xie, Porous polymer monoliths: an alternative to classical beads, Adv. Biochem. Eng. Biotechnol. 76 (2002) 88–123.
[19] E.C. Peters, M. Petro, F. Svec, J.M.J. Fréchet, Molded rigid polymer monoliths as separation media for capillary electrochromatography, Anal. Chem. 69 (1997) 3646–3649.
[20] F. Svec, E.C. Peters, D. Sýkora, G. Yu, J.M.J. Fréchet, Monolithic stationary phases for capillary electrochromatography based on synthetic polymers: Designs and applications, J. High Resolut. Chromatogr. 23 (2000) 3–18.
[21] F. Svec, Capillary column technology: continuous polymer monoliths, in: Z. Deyl, F. Svec, Capillary Chromatography, Elsevier, Amsterdam, 2001, pp. 183–240.
[22] F. Svec, Capillary electrochromatography: a rapidly emerging separation method, Adv. Biochem. Eng. Biotechnol. 76 (2002) 1–47.

[23] S. Zeng, C.-H. Chen, J.G. Santiago, J.-R. Chen, R.N. Zare, J.A. Tripp, F. Svec, J.M.J. Fréchet, Electroosmotic flow pumps with polymer frits, Sens. Actuators B: Chem. 82 (2002) 209–212.
[24] M. von Smoluchowski, M. Graetz, Handbuch der Elektrizität und des Magnetisms, von Johann Ambrosius Barth Verlag, Lepzig, 1921.
[25] C.L. Rice, R. Whitehead, Electrokinetic flow in a narrow cylindrical capillary, J. Phys. Chem. 69 (1965) 4017–4024.
[26] J.A. Tripp, F. Svec, J.M.J. Fréchet, Grafted macroporous polymer monolithic disks: a new format of scavengers for solution-phase combinatorial chemistry, J. Comb. Chem. 3 (2001) 216–223.
[27] S. Yao, D.E. Hertzog, S. Zeng, J.C. Mikkelsen Jr., J.G. Santiago, Porous glass electroosmotic pumps: design and experiments, J. Colloid Interface Sci. 268 (2003) 143–153.
[28] J.A. Tripp, J.A. Stein, F. Svec, J.M.J. Fréchet, Reactive filtration: use of functionalized porous polymer monoliths as scavengers in solution-phase synthesis, Org. Lett. 2 (2002) 195–198.
[29] J.A. Tripp, F. Svec, J.M.J. Fréchet, Solid-phase acylating reagents in new format: Macroporous polymer disks, J. Comb. Chem. 3 (2001) 604–611.
[30] Hunter, R.J., Zeta Potential in Colloidal Science: Principles and Applications, Academic Press, London, 1981.